

**Noise amplification precedes extreme epileptic events on human EEG**

Oleg E. Karpov,<sup>1</sup> Vadim V. Grubov,<sup>2,3</sup> Vladimir A. Maksimenko<sup>2,3</sup>, Nikita Utashev<sup>1</sup>, Viachaslav E. Semerikov<sup>2</sup>, Denis A. Andrikov<sup>2</sup> and Alexander E. Hramov<sup>3</sup>

<sup>1</sup>*National Medical and Surgical Center named after N. I. Pirogov, Ministry of Healthcare of the Russian Federation, 105203 Moscow, Russia*

<sup>2</sup>*Research and Production Company “Immersmed”, Moscow 105203, Russia*

<sup>3</sup>*Neuroscience and Cognitive Technology Laboratory, Center for Technologies in Robotics and Mechatronics Components, Innopolis University, 420500 Kazan, Russia*



(Received 21 June 2020; revised 15 January 2021; accepted 19 January 2021; published 11 February 2021)

Extreme events are rare and sudden abnormal deviations of the system’s behavior from a typical state. Statistical analysis reveals that if the time series contains extreme events, its distribution has a heavy tail. In dynamical systems, extreme events often occur due to developing instability preceded by noise amplification. Here, we apply this theory to analyze generalized epileptic seizures in the human brain. First, we demonstrate that the time series of electroencephalogram (EEG) spectral power in a frequency band of 1–5 Hz obeys a heavy-tailed distribution, confirming the presence of extreme events. Second, we report that noise on EEG signals gradually increases before the seizure onset. Thus, we hypothesize that generalized epileptic seizures in humans are the extreme events emerging from instability accompanied by preictal noise amplification similar to other dynamical systems.

DOI: [10.1103/PhysRevE.103.022310](https://doi.org/10.1103/PhysRevE.103.022310)

**I. INTRODUCTION**

Extreme events are sudden abnormal deviations of the system’s behavior from a typical state, which are observed very rarely in time [1–3]. Numerous studies discovered this phenomenon in a wide range of models and real-life systems.

Researchers theoretically and numerically examined different scenarios describing the occurrence of extreme events in model systems, including coupled oscillators and complex networks [1,4,5], fluids [6], nanophotonics [7], and optical complex systems [8,9].

Along with the models, extreme events occur in real-world systems and, sometimes, harm human life. Such extreme events include traffic jams in transportation networks, floods in rivers, power blackouts in power grids, severe rains, economic crises, tsunamis, killer waves in the ocean, etc.

Recently, scientists started considering spontaneous bursting activity in neuronal populations as extreme events [10,11]. In this context, they especially highlight epileptic seizures as the brightest manifestation of extreme behavior in the neural network of the brain [3,11–15].

An epileptic seizure is a sudden malfunction of the brain caused by excessive and hypersynchronous neuron activity in the brain neuronal network. Sometimes, seizures may occur due to brain injury, stroke, tumor, or congenital disabilities [16,17]. However, in most cases, the exact reason remains unknown.

The epileptic seizures may be focal and generalized [18]. Focal seizures originate from a circumscribed part of the brain. In contrast, generalized seizures involve bilaterally and synchronously two hemispheres, if not the entire cortex. Generalized seizures have an evident electroencephalo-

graphic hallmark—a synchronization of noninvasive [electroencephalogram (EEG)] or invasive [electrocorticogram (ECoG)] signals recorded in different, even very distant, brain areas. At the same time, surprisingly little is known about the fundamental mechanisms of their onset.

Extreme event theory may provide insight into the possible onset mechanisms [3,19]. Like in other fields, ongoing extreme events in the brain probably change the properties of time series, e.g., EEG or ECoG signals, beforehand. It enables revealing earlier manifestations of ongoing seizures from preictal EEG, as had been done to predict other extreme events, e.g., rainfalls. However, the application of extreme event theory to epilepsy remains in its startup phase [12,15].

In our recent paper [20] we applied extreme event theory to analyze ECoG recordings of rats with a genetic predisposition to absence epilepsy. We reported that absence seizures induced a drastic increase of wavelet power (WP) in a frequency range of 6–8 Hz. In this frequency range, WP time series demonstrated extreme-events-related properties, while for other frequencies, there were no manifestations of the extreme behavior. We further observed that in this frequency range WP exhibits long-range correlations. The uncovered long-range correlation is inherent in systems near a critical point [21], where small fluctuations grow due to increasing instability. This effect, known as prebifurcation signal (noise) amplification, has been observed earlier in physical, ecological, and biomedical systems (see Refs. [22–25]).

We hypothesize that the epileptic seizures, like other extreme events, may onset through the instability. Therefore, the noise intensity should increase during the preictal period. To validate this hypothesis, we considered human EEG signals

during secondary generalized epilepsy. Similarly to the previous work, we defined a frequency band of epileptic activity and reported extreme behavior manifestation. We considered a preictal state and found a gradually increasing noise intensity prior to approaching seizure onset. These results complement our knowledge about epileptic seizures as extreme events and advance understanding of possible mechanisms leading to extreme behavior in the brain.

## II. MATERIALS AND METHODS

### A. Experimental data

In the present work we studied EEG data of ten patients with generalized epilepsy (age, 21–53 years; gender, six male and four female). Continuous 24-h EEG and video monitoring during sleep and wakefulness was performed for these patients. The goal of this medical procedure was registration of epileptic activity and verification of epileptogenic zones for further clinical treatment. All medical procedures were held in the Laboratory for Diagnosis and Treatment of Epilepsy, National Medical and Surgical Center named after N. I. Pirogov (Moscow, Russia), in accordance with the Helsinki Declaration and were approved by the local ethics committee. During monitoring, patients kept a regular daily routine with occasional physiological trials (such as photic stimulation and hyperventilation) that are standard for such a medical procedure. Each patient had from one to four epileptic seizures during the time of the monitoring, namely, two out of ten patients had four seizures, two patients had three seizures, two patients had two seizures, and four patients had only one seizure. While all the patients were subjected to physiological trials, none of the seizures was triggered by photic stimulation or hyperventilation; i.e., all epileptic seizures were spontaneous. To be able to compare the patients with different numbers of seizures we averaged obtained results over all occurred seizures for each patient.

### B. Experimental equipment

A “Micromed” encephalograph (Micromed S.p.A., Italy) was used for EEG recording. EEG signals were recorded for 25 channels according to the international “10-20” system with a ground electrode placed on the forehead and reference electrodes placed at the ears. For EEG signal recording, “Natus neurologi” gold EEG cup electrodes with 10 mm diameter were used. To increase the skin conductivity EEG electrodes were placed using Ten20 conductive gel. After the electrodes were placed, the impedances were monitored to get the best possible quality of EEG recordings. Common impedance values were 10–50 k $\Omega$ , which is sufficient for long-term EEG monitoring. EEG signals were recorded with sampling rate of 128 Hz.

A video monitoring system was used to monitor patients’ states for easier analysis and segmentation of experimental data.

### C. Data acquisition and preprocessing

Acquired experimental EEG data and video records were examined and marked by experienced neurophysiol-

ogists. Marking includes information on epileptic seizures (onset/offset, conditions, corresponding video record) and physiological tests (photic stimulation, hyperventilation). We used this marking to form EEG trials corresponding to the different experimental conditions.

It is well known that EEG data (especially during long-term recording) are exposed to the influence of various external and internal noises. External noises may be caused by poor contact of EEG electrodes, loose wires, the power network, etc. Internal noises (or physiological artifacts) originate from physiological processes such as heartbeat, blinking, or muscle activity [26,27]. One of the basic (and the most simple) ways to deal with noises and artifacts is EEG data filtration. A proper filter can help to eliminate (or at least diminish) the influence of some low-frequency noises (for example, noises from stray effects or cardiac rhythms) and some high-frequency noises (a 50-Hz component of the power network, part of muscle activity artifacts, etc.). In our study, we used a bandpass filter with cutoff frequencies of 1 and 60 Hz and a 50-Hz notch filter.

However, the frequency range of some artifacts (such as blinking) overlaps an effective frequency range of EEG signals. To remove these artifacts, we used independent component analysis (ICA). ICA allows us to decompose the studied set of EEG data into several independent components [28,29]. In ICA application to blinking artifact removal, one should search for the component that contains these artifacts. It can be safely assumed that eye movements are independent of electrical brain activity, so components with eye-movement artifacts will be independent of the other components with EEG signals. Thus, by deleting the component with artifacts and reconstructing EEG signals with the rest of the components, one can obtain an EEG data set with removed blinking artifacts.

### D. Time-frequency analysis

For time-frequency analysis of EEG data we used continuous wavelet transform (CWT) [30,31]. This approach is widely used for analysis of complex nonstationary signals with multiple rhythmic components in systems of different nature, including biological ones [32–34]. The CWT is defined as convolution of studied signal  $x(t)$  with set of wavelet basis functions  $\varphi_{s,\tau}$ :

$$W_n(s, \tau) = \frac{1}{\sqrt{s}} \int_{-\infty}^{\infty} x_n(t) \varphi_{s,\tau}^*(t) dt, \quad (1)$$

where  $n = 1, 2, \dots, N$  is the number of the EEG channel ( $N = 25$ ) and \* stands for complex conjugation. Each basis function  $\varphi_{s,\tau}$  can be obtained from the same original function  $\varphi_0$ , known as a mother wavelet:

$$\varphi_{s,\tau}(t) = \frac{1}{\sqrt{s}} \varphi_0\left(\frac{t-t_0}{s}\right), \quad (2)$$

where  $s$  is a time scale defining expansion and compression of the mother wavelet and  $t_0$  is the time shift of the mother wavelet. In the present study, we used a complex Morlet wavelet as the mother wavelet:

$$\varphi_0(\eta) = \pi^{-\frac{1}{4}} e^{j\omega_0\eta} e^{-\frac{\eta^2}{2}}, \quad (3)$$

where the parameter  $\omega_0 = 2\pi$  is the central frequency of the Morlet wavelet,  $\eta = (t - t_0)/s$ . In order to interpret results of the CWT, wavelet scales  $s$  can be converted into the Fourier frequencies  $f$  as follows:

$$f = \frac{\omega_0 + \sqrt{\omega_0^2 + 2}}{4\pi s}. \quad (4)$$

The value of the central frequency  $\omega_0 = 2\pi$  is commonly used, as it leads to a simple relation between the wavelet scales  $s$  and the Fourier frequencies  $f$ , namely,  $f \approx 1/s$ . This relation allows a clearer representation of the results along with the possibility to compare estimations performed by means of CWT and other numerical techniques.

In the present work we analyzed the WP  $E(f, \tau) = |W(f, \tau)|$ . The values of  $E(f, \tau)$  were averaged over all EEG channels and over the frequency bands of interest: 1–5 Hz and 5–10 Hz. The normalized wavelet power (NWP) was the WP normalized over the average WP for each subject.

The wavelet analysis of EEG recordings was performed with developed C/CUDA software for increasing computation performance [35].

### E. Probability density function and its approximation

To construct a probability density function (PDF), we extracted all local maxima on WP time series and normalized them by a global maximum. According to the extreme value theory, namely, the Fisher-Tippett-Gnedenko theorem [36], obtained PDFs should be close to the Gumbel, Fréchet, or Weibull distribution. Our previous studies on absence epilepsy in WAG/Rij rats suggest that the Weibull distribution is more suitable for this task. For example, in Ref. [20] we showed that experimental PDFs for both normal and epileptic activity can be fitted by Weibull distributions with drastically different parameters. Thus, in the present work PDFs for background and pathological EEG were fitted by exponentiated Weibull distribution [37]. The PDF for the exponentiated Weibull distribution is

$$f(x, a, c) = ac[1 - \exp(-x^c)]^{a-1} \exp(-x^c)x^{c-1}, \quad (5)$$

where  $a$  is the exponentiation parameter, with the special case  $a = 1$  corresponding to the (nonexponentiated) Weibull distribution and  $c$  is the shape parameter of the nonexponentiated Weibull law ( $x > 0$ ,  $a > 0$ ,  $c > 0$ ). The probability density in Eq. (5) is defined in the “standardized” form. To shift and/or scale the distribution, additional parameters can be used: *loc* and *scale*, correspondingly. The *loc* parameter reflects the shift of the distribution with fixed parameters  $a$  and  $c$  across the axis of NWP: higher values of *loc* shift distribution to the higher values of NWP. The *scale* parameter marks the expansion and compression of the initial distribution: positive values of *scale* correspond to expansion, while negative values correspond to compression of the Weibull distribution. Thus, there are overall four parameters for exponentiated Weibull distribution.

We tested goodness of fit to be sure that the exponentiated Weibull distribution is appropriate to fit the studied experimental data. We used the  $\chi^2$  test and G test. A  $\chi^2$  test is a statistical hypothesis test that is valid to perform when the test

statistic is  $\chi^2$  distributed under the null hypothesis, specifically Pearson’s  $\chi^2$  test and variants thereof. Pearson’s  $\chi^2$  test is used to determine whether there is a statistically significant difference between the expected frequencies and the observed frequencies in one or more categories of a contingency table. In the standard applications of this test, the observations are classified into mutually exclusive classes. If the null hypothesis is true, the test statistic computed from the observations follows a  $\chi^2$  frequency distribution. The purpose of the test is to evaluate how likely the observed frequencies would be, assuming the null hypothesis is true. G tests are likelihood-ratio or maximum-likelihood statistical significance tests that are increasingly being used in situations where  $\chi^2$  tests were previously recommended.

To fit experimental PDFs with exponentiated Weibull distribution and to perform goodness of fit tests we used the SCIPY library from PYTHON, namely, the special module Statistical functions (`scipy.stats`). The function `stats.exponweib.fit` was applied to PDF data; it returns maximum-likelihood estimations for *a*, *c*, *loc*, and *scale* parameters of the Weibull distribution from data (PDF). The function `stats.chisquare` was used to calculate a one-way  $\chi^2$  test. The function `stats.power_divergence` was used to perform the Cressie-Read power divergence statistic and goodness of fit test. The parameter *lambda* = 0 corresponded to “log-likelihood” ratio, also known as the G test.

### F. Noise intensity estimation

In various systems, including the brain, the noise component is often represented by  $1/f$  noise (or flicker noise) [38–40]. The spectral density law of this type of noise corresponds to the power law or, more specifically,

$$S(f) = C/f^\alpha, \quad (6)$$

where  $C$  is a constant factor,  $f$  reflects frequency, and  $\alpha$  defines a flicker noise parameter. We can use the power spectrum  $S(f)$  plotted in logarithmic coordinates to estimate the flicker noise. In this case, the logarithmic transform renders the  $C/f^\alpha$  power spectrum in a straight line whose slope,  $-\alpha$ , can be easily estimated.

To estimate the noise intensity, we calculated wavelet spectra for the corresponding time intervals in the frequency range  $F \in [1, 30]$  Hz, common for EEG studies. These spectra were plotted in a logarithmic scale and fitted with a power law. For all analyzed EEG intervals, the fitted power law leaned towards the  $S(f) = C/f^\alpha$  form, thus marking the presence of  $1/f$ -type noise. Then, we estimated noise intensity  $I$  as an integral:

$$I = \int_{f \in F} C/f^\alpha df. \quad (7)$$

We suggested that characteristic  $I$  can be used to reflect overall noise intensity on analyzed EEG signals.

The function `curve_fit` in PYTHON was applied to wavelet spectra. It uses nonlinear least squares to fit a function (power law) to data (wavelet spectra) and returns values of  $\alpha$  and  $C$  parameters of the fitted power law.

### G. Signal variance estimation

Increasing signal variance is known to be one of the early warnings for critical transitions [41]. For signal variance estimation in studies on preictal EEG activity, unbiased sample variance  $s^2$  can be used [42].

We calculated unbiased sample variance as follows:

$$s_{n,T}^2 = \frac{1}{m-1} \sum_{i=1}^m (x_i - \bar{x}), \quad (8)$$

where  $n = 1, 2, \dots, N$  is the number of the EEG channel ( $N = 25$ ) and  $T$  is the analyzed time window from EEG data,  $m = 3840$  is the number of values in the sample (time window),  $x$  is the studied signal in the time window, and  $\bar{x}$  is the mean value of  $x$  in this window. The factor  $1/(m-1)$  appears instead of  $1/m$  because of Bessel's correction.

We evaluated unbiased sample variance  $s^2$  on EEG signals filtered with a Butterworth filter in the frequency range 1–30 Hz. For this we used the SCIPY library from PYTHON, namely, the module signal processing (`scipy.signal`) and its function `signal.butter`.

We calculated unbiased sample variance  $s^2$  for each EEG channel in each analyzed time window. Values of unbiased sample variance  $s^2$  were averaged across all EEG channels to obtain a single value for each analyzed time window.

### H. Experimental conditions

In this work, we tested two hypotheses in the framework of the within-subject design. First, we tested a difference in the PDF between the baseline EEG (normal activity) and epileptic seizures (extreme events). For this purpose, we introduced two experimental conditions: seizure and baseline. The first condition included all epileptic seizures (from one to four, depending on the patient's data). The second condition comprised  $\sim 4$  h of baseline recording and included ten short 1500-s segments randomly chosen across the data. In both conditions, we fitted the data with the Weibull distribution. The  $\chi^2$  test and/or G test provided  $p > 0.99$  for all patients.

Second, we tested changes in noise intensity during the preictal period. For this purpose, we introduced four experimental conditions,  $T_1, \dots, T_4$ , before each epileptic seizure. First, we placed a 30-s length window right before the seizure onset  $T_0$ , forming the condition  $T_4 \in [T_0 - 30, T_0]$  s. Then, we shifted the window by 15 s to the left, forming the condition  $T_3 \in [T_0 - 45, T_0 - 15]$  s. These actions were repeated for the next two steps, providing the condition  $T_2 \in [T_0 - 60, T_0 - 30]$  s and the condition  $T_1 \in [T_0 - 75, T_0 - 45]$  s. In all four experimental conditions, we calculated noise intensity. For each subject, we averaged these values across the seizures.

## III. RESULTS

### A. Results of time-frequency analysis

First, we analyzed the time-frequency structure of EEG signals and specified the frequency band of interest. Having considered EEG segments containing epileptiform activity [Fig. 1(a)], we observed that the central frequency of the epileptic discharges lies in the frequency range 1–5 Hz for the

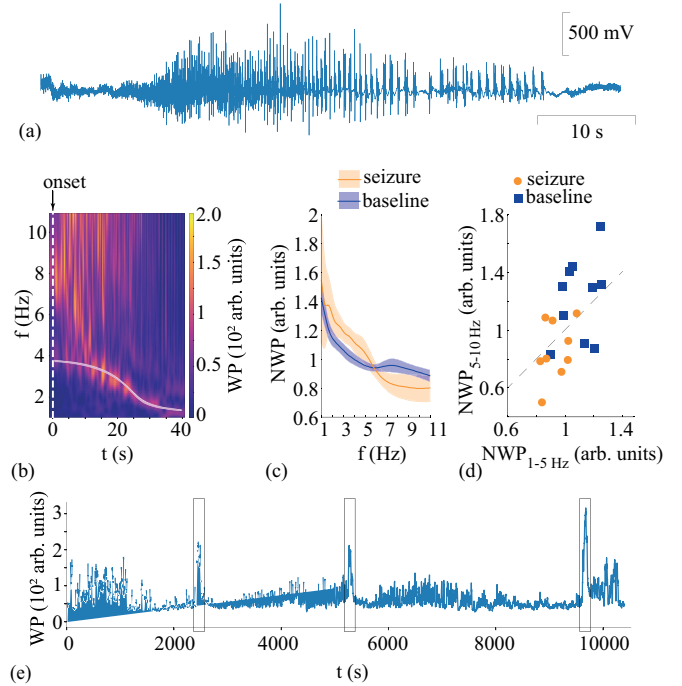


FIG. 1. Wavelet power. (a) The fragment of the EEG signal registered from the frontal electrode, Fp2, representing epileptic seizure. (b) The time-frequency evolution of the WP during the seizure. The vertical dashed line shows the seizure onset, and a solid curve follows the frequency with the highest WP (a wavelet skeleton). (c) NWP corresponding to the epileptic seizure and the baseline. Data are shown as the group mean  $\pm$  SE (Standard Error). (d) The pairwise difference distribution between NWP in the frequency bands of 1–5 Hz and 5–10 Hz. The dashed line corresponds to the equality of the NWP in these frequency bands. The circles and squares reflect the individual subjects' NWP for the seizure and the baseline. (e) The time series illustrate the WP evolution in the 5–10 Hz frequency band in the course of the experiment. The sharp peaks reflect the seizures and are considered extreme events.

most patients. Figure 1(b) demonstrates the WP for a typical epileptic seizure averaged over all 25 EEG channels. The solid curve in Fig. 1(b) follows the oscillatory component, which starts from 4–5 Hz at the seizure onset and decreases to  $\sim 1$  Hz in the course of the seizure duration. We contrasted the NWP during the epileptic seizure to the baseline [Fig. 1(c)]. As a result, the mean NWP in the frequency band 1–5 Hz was higher during the seizure.

In contrast, the mean NWP in the frequency band 5–10 Hz peaked during the baseline. Figure 1(d) demonstrates the comparison between the mean NWP in the frequency bands 1–5 Hz and 5–10 Hz. The dashed line in Fig. 1(d) corresponds to the equality of the NWP in these frequency bands. The circles and squares reflect the individual subjects' NWP for the seizure and the baseline. One can see that the squares appear above the dashed line for seven subjects, manifesting that the 5–10 Hz NWP exceeds the 1–5 Hz NWP. In contrast, the circles appear below the dashed line for seven subjects, manifesting that the 1–5 Hz NWP exceeds the 5–10 Hz NWP. Thus, the seven subjects exhibit higher 1–5 Hz NWP during the seizure and higher 5–10 Hz NWP during the baseline.

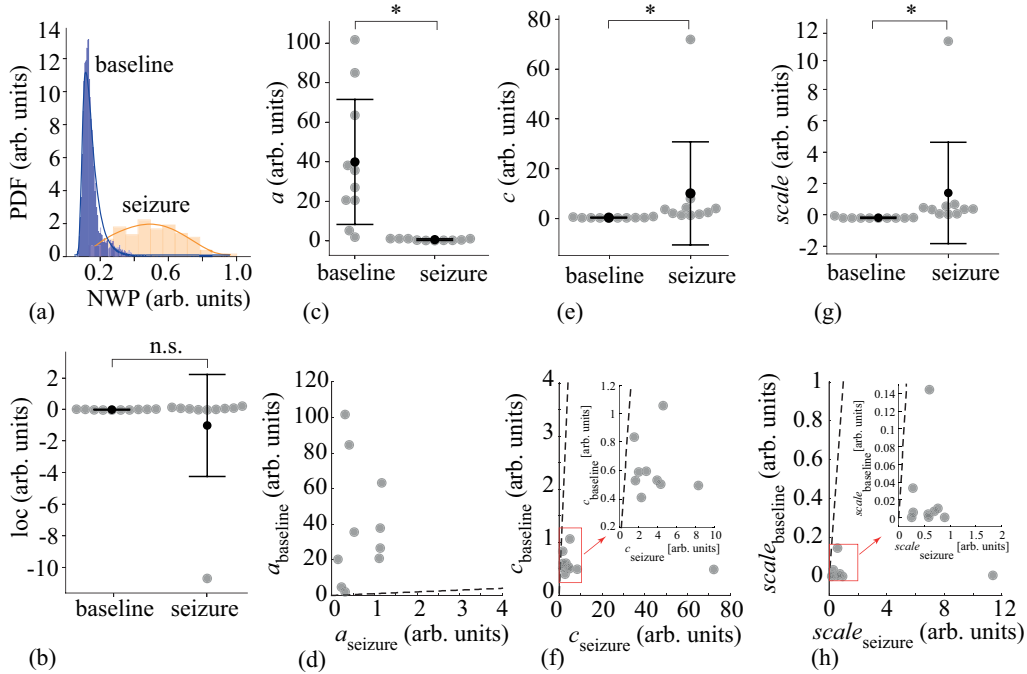


FIG. 2. (a) The PDF of the local maxima of NWP in the 1–5 Hz frequency band and its Weibull approximation. Data are shown for a single subject. The Weibull parameters of the seizure and baseline: (b) localization parameter *loc* [mean  $\pm$  standard deviation (SD),  $p = 0.74$ , Wilcoxon test], (c) exponentiation parameter *a* (mean  $\pm$  SD,  $p = 0.005$ , Wilcoxon test) and (d) its pairwise differences distribution, (e) shape parameter *c* (mean  $\pm$  SD,  $p = 0.005$ , Wilcoxon test) and (f) its pairwise differences distribution, and (g) scaling parameter *scale* (mean  $\pm$  SD,  $p = 0.005$ , Wilcoxon test) and (h) its pairwise differences distribution. The dashed line in (d), (f), and (h) reflects the Weibull parameter’s equality for the seizure and baseline. Points to the right of this line indicate that the Weibull parameter is higher during the seizure, and vice versa.

To analyze epileptic activity, we defined the frequency band of interest as 1–5 Hz and considered WP averaged over this band. Figure 1(e) shows a long-term time series of WP with vast segments of background activity and short episodes of epileptic seizures (shown by frames). The epileptic activity demonstrates generally higher maxima of WP. We noted that WP in the 5–10 Hz range might be relatively high outside epileptic seizures, e.g., during sleep. At the same time, WP during sleep was represented by scarce maxima with noticeable drops in WP between them. In epileptic seizures, high WP was more consistent and formed a distinctive pattern on time series.

**B. PDFs of baseline and seizure**

We collected all local maxima on the WP time series in the 1–5 Hz frequency band and fitted their PDF with Weibull distribution (see Materials and Methods). Figure 2(a) shows the illustrative PDFs of a single patient for baseline activity and epileptic seizures. The histograms show experimental data (blue for the baseline and orange for epileptic seizures), and the lines reflect fitted data.

The presented data show evidence that the baseline PDF differs from the PDF obtained for epileptic activity. In the former case, the PDF peaks at low values of NWP. In the latter case, the PDF spreads across the broader range of NWP and forms a heavy-tailed distribution.

We contrasted the parameters of the Weibull distribution during baseline and seizure. According to the Shapiro-Wilk test, the distribution of Weibull parameters across participants was not normal ( $p > 0.05$ ). Therefore, we applied a nonparametric Wilcoxon signed-rank test to compare them between baseline and seizure.

As a result, the localization parameter *loc* did not change between seizure (Mdn = 0.08, IQR = 0.09) and baseline (Median = 0.02, IQR = 0.04):  $Z = -1.78$ ,  $p = 0.74$  [Fig. 2(b)].

The exponentiation parameter *a* for seizure (Mdn = 0.46, IQR = 0.81) was significantly lower than for baseline (Mdn = 31.33, IQR = 36.61):  $Z = -2.8$ ,  $p = 0.005$  [Fig. 2(c)]. Analysis of the pairwise differences revealed that all subjects demonstrated an effect in the same direction as the group [Fig. 2(d)]. The dashed line in Fig. 2(d) illustrates the case when  $a_{\text{baseline}} = a_{\text{seizure}}$ . All points that reflect individual subjects’ values appear above this line, manifesting  $a_{\text{baseline}} > a_{\text{seizure}}$ .

The shape parameter *c* for seizure (Mdn = 3.32, IQR = 2.43) exceeded the one for baseline (Mdn = 0.53, IQR = 0.09):  $Z = -2.8$ ,  $p = 0.005$  [Fig. 2(e)]. Analysis of the pairwise differences also revealed that all subjects demonstrated an effect in the same direction as the group [Fig. 2(g)]. Namely, all points in Fig. 2(g) appear below the dashed line indicating that  $c_{\text{baseline}} < c_{\text{seizure}}$ .

Finally, scaling parameter *scale* for seizure (Mdn = 0.57, IQR = 0.39) exceeded the one for baseline (Mdn = 0.006,

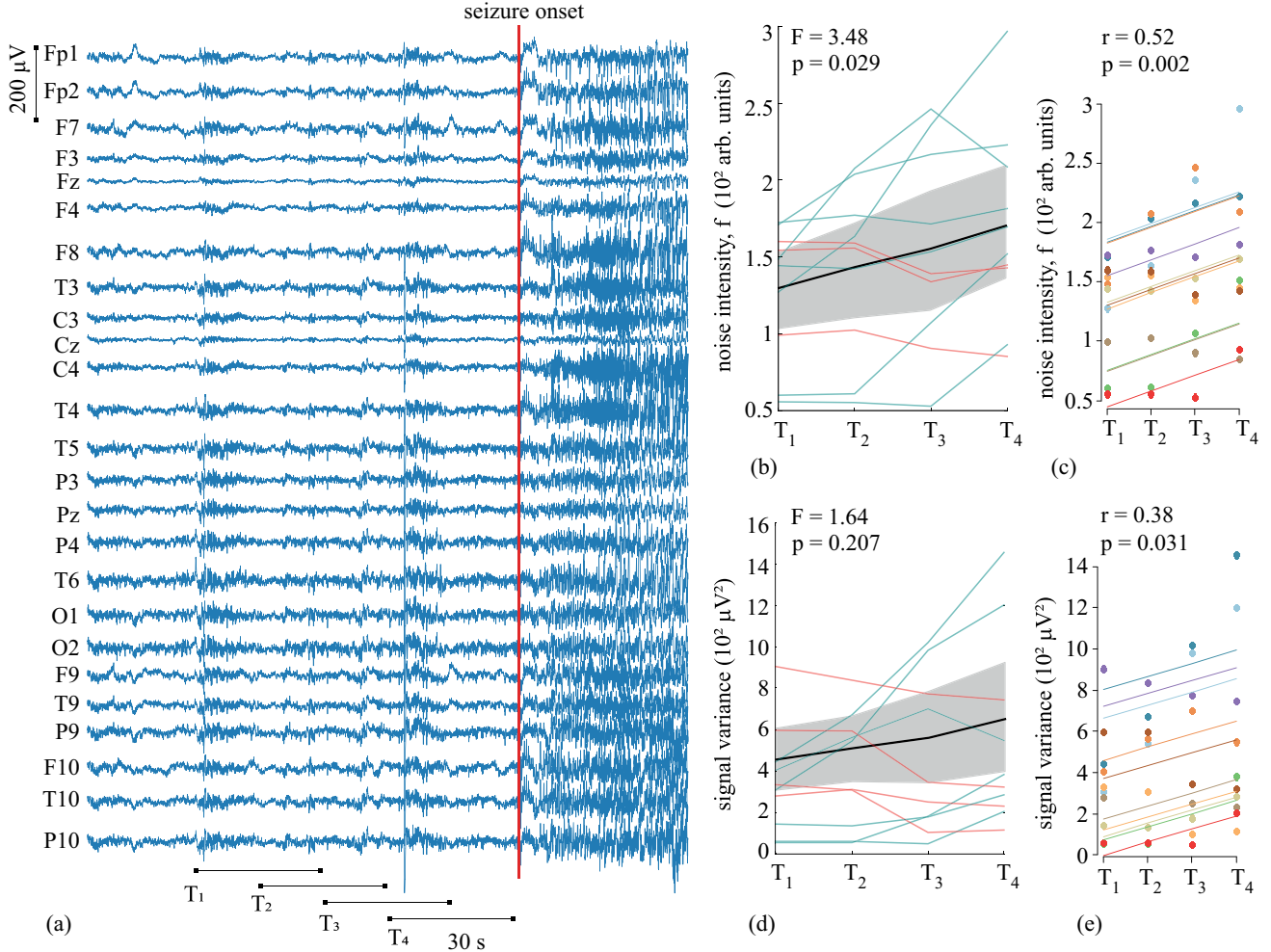


FIG. 3. (a) The set of EEG signals, including the preictal period and the onset of the epileptic seizure (vertical solid line). The four horizontal lines,  $T_1, \dots, T_4$ , show positions of the time windows used for the noise intensity estimation. Each window's length is equal to 30 s. (b) The noise intensity (mean  $\pm$  95% confidence interval and individual values) estimated for these time windows,  $F(3, 27) = 3.48$ ,  $p = 0.0029$  via one-way analysis of variance (ANOVA). (c) The regression plot: colored dots correspond to each participant's data, lines have a similar slope,  $r = 0.52$  estimated for these participants via correlation analysis with repeated measures ( $p = 0.002$ ). (d) The signal variance (mean  $\pm$  95% confidence interval and individual values) calculated for these time windows,  $F(3, 27) = 1.64$ ,  $p = 0.207$  via one-way ANOVA. (e) The regression plot: colored dots correspond to each participant's data, lines have a similar slope,  $r = 0.38$  estimated for these participants via correlation analysis with repeated measures ( $p = 0.031$ ).

IQR = 0.007):  $Z = -2.8$ ,  $p = 0.005$  [Fig. 2(g)]. Analysis of the pairwise differences also proved that all subjects demonstrated the effect in the same direction as the group [all points in Fig. 2(h) appear below the dashed line].

### C. Noise on EEG signals increases preictally

In the previous section, we demonstrate that the time series of EEG spectral power in the 1–5 Hz frequency band forms a heavy-tailed distribution. We suppose that a heavy tail reflects the presence of epileptic seizures producing a dramatic increase of 1–5 Hz spectral power. The fact that seizures satisfy an extreme-event definition suggests a possible onset mechanism based on dynamical systems theory. As we know from the dynamical systems analysis, extreme events arise due to the instability. In the vicinity of this unstable point, the system state exhibits the amplification of the small perturbations.

On the EEG signals, these small perturbations may represent the noise originating from the neuronal activity. Thus, if the extreme epileptic event onsets are due to instability, its development should accompany the noise amplification during a preictal state.

We compare the noise intensity values on the four windows ( $T_1, \dots, T_4$ ) during the preictal state [see Fig. 3(a)]. The distribution of noise intensity across the subjects was normal for each window ( $p > 0.05$  via the Shapiro-Wilk test). An ANOVA with a window serving as a within-subject factor revealed a significant main effect:  $F(3, 27) = 3.48$ ,  $p = 0.029$ . Figure 3(b) shows that the mean noise intensity increases when the window shifts toward the seizure onset.

Visual inspection of the individual values showed evidence that seven subjects followed the group tendency exhibiting the growth of the noise intensity (green lines). The noise intensity decreased towards the seizure onset for three subjects, but

with the lower slope (red lines). To quantify the relationship between the window number and noise intensity at the group level, we applied correlation analysis with the repeated measures [43]. It is a statistical technique for determining the common within-individual association for paired measures (the noise intensity and the window number) assessed on two or more occasions ( $T_1, \dots, T_4$ ) for multiple individuals. As a result, we observed a moderate positive relationship:  $r_{rm}(29) = 0.52$ , 95% CI [0.20, 0.74],  $p = 0.002$ . Figure 3(c) presents the results for the correlation analysis. The dots of different color show the noise intensity estimated for the single subject for all windows. The colored lines have a similar slope estimated for these participants at the group level. After a visual inspection of these data, one can see that the points (e.g., brown ones) do not agree with the line fit for some subjects. Similarly to Fig. 3(c), it refers to the subjects that do not follow the group mean tendency. Simultaneously, the significance level of  $p = 0.002$  allows us to conclude that the obtained correlation model describes the group data.

We also compare the signal variance on the four windows ( $T_1, \dots, T_4$ ). Figure 3(d) shows that the mean signal variance increases when the window shifts toward the seizure onset. Similarly to the noise intensity, there are subjects for which the variance decreases. An ANOVA with a window serving as a within-subject factor revealed an insignificant main effect:  $F(3, 27) = 1.64$ ,  $p = 0.207$ . That means that between-subject variability exceeds the change of the signal variance between the windows ( $T_1, \dots, T_4$ ). In contrast, correlation analysis with repeated measures revealed a moderate positive relationship:  $r_{rm}(29) = 0.38$ , 95% CI [0.20, 0.74],  $p = 0.031$  [Fig. 3(e)].

Thus, the majority of subjects exhibited growth of the noise intensity and variance before the seizure. At the same time, several participants demonstrated an effect in the opposite direction. To test whether the change in noise intensity and the signal variance correlate, we used correlation analysis with the repeated measures. It demonstrated a strong positive relationship:  $r_{rm}(29) = 0.809$ , 95% CI [0.62, 0.9],  $p = 3.5 \times 10^{-8}$  (Fig. 4).

#### IV. DISCUSSION AND CONCLUSION

We consider noninvasive EEG signals of human participants with generalized epileptic seizures. We show that the PDF of the baseline EEG wavelet power peaks at low values. In contrast, the same PDF for epileptic seizure expands across the broader range and forms a heavy-tailed distribution. According to the extreme value theory (the Pickands-Balkema-de Haan theorem [44,45]), the long tail reflects extreme behavior. We successfully fit this tail with the heavy-tailed Weibull distribution, as we did earlier for epileptic rats [20], confirming that generalized epileptic seizures in humans are a sort of extreme event.

In dynamic systems, extreme events may appear through different scenarios, e.g., imperfect phase synchronization and saddle-type equilibrium [46] or attractor bubbling and noise-induced transitions [1]. In the latter case, occasional noise-induced jumps cause the system to irregularly and briefly leave the vicinity of an invariant manifold containing a chaotic attractor. During these occasions, the system state

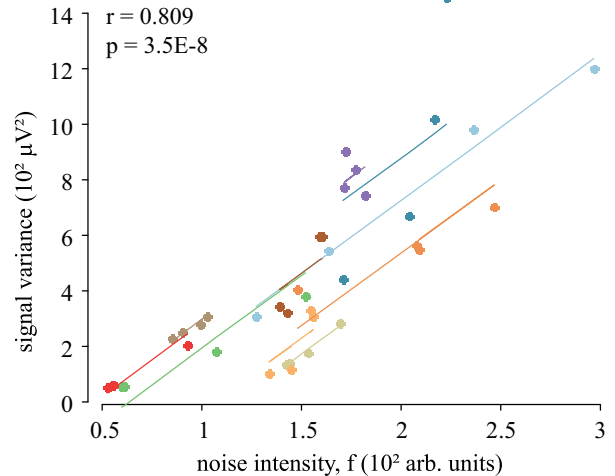


FIG. 4. The regression plot: colored dots correspond to each participant's data (noise intensity and signal variance); lines have a similar slope, reflecting a strong positive correlation ( $r = 0.809$ ) between the noise intensity and signal variance estimated for these participants via correlation analysis with repeated measures.

follows an orbit that moves away from the invariant manifold but eventually returns to the attractor. In this notation, extreme events reflect the episodes when the system state travels to phase space regions far from the invariant manifold.

Another view is that the on-off intermittency in the system can lead to attractor bubbling. Pisarchik and colleagues reported this scenario for rogue waves in an erbium-doped fiber laser driven by harmonic pump modulation [47]. In their system, low-frequency noise in a diode pump current led to rare jumps to rogue waves, the extreme events with high-amplitude pulses. Soli and co-authors obtained similar results on rogue optical waves in Ref. [48].

According to our previous studies [49,50], the distribution of return times  $\tau$  for epileptic seizures in an animal model of epilepsy obeys a power law  $p \sim \tau^\gamma$ ,  $\gamma = -3/2$ , manifesting on-off intermittency. In their work [51], Suffczynski and colleagues also reported that the occurrence of epileptic seizures had some periodicity and supposed that noise may cause transitions between states.

We considered these results in Ref. [20] and proposed that the brain can demonstrate prebifurcation signal (noise) amplification near the onset of an epileptic seizure, like many other dynamical systems in the vicinity of a critical point [21,23–25]. We considered interictal and preictal states on the EEG signal to reveal this phenomenon in the long-term epileptic EEG of WAG/Rij rats. We found that a PDF of 6–8 Hz wavelet power changed even before the seizure onset, and suggested applying this phenomenon to predict seizures.

We suppose that similar dynamical mechanisms may describe the onset of absence seizures in rats and generalized seizures in humans. However, epileptic seizures are more sparse for human patients than for animal models of epilepsy (e.g., the WAG/Rij rats strain): most human EEG recordings lasted for several days and contained up to four seizures.

In this study, we have insufficient amounts of ictal states to analyze return times and long-range correlations. Nevertheless, we can compare the Weibull approximation of interictal

and preictal PDFs. We show that the Weibull approximation of interictal PDFs has a relatively high exponentiation parameter while shape and scale parameters are low. Therefore, the PDF peaks at a small wavelet power value with no noticeable tail. For the ictal PDF, the Weibull approximation has the lowest exponentiation parameter and the highest shape and scale parameters, indicating a broader distribution with a heavy tail.

These features of the Weibull approximation are comparable to those obtained for seizures in rats. Since the correlation analysis and on-off intermittency in rats' EEGs offer a noise-related mechanism of extreme event onset, we suppose increasing noise may precede seizures in humans. Analysis of the preictal state reveals a gradually growing noise intensity, confirming our hypothesis. To estimate noise intensity, we fitted a wavelet power spectrum with a  $C/f^\alpha$  distribution and integrated it in the frequency range 1–30 Hz. In this way, increasing noise intensity may accompany the growth of the total signal power. A similar concept of growing signal energy before seizure was shown by Litt *et al.* [52]. They analyzed long (up to 14 days) intracranial EEG recordings from five patients with temporal lobe epilepsy and obtained that the accumulated energy increased in the 50 min before seizure onset, compared to baseline. At the same time, Harrison *et al.* did not confirm these results [53]. They considered the accumulated energy and windowed average power in the a single channel of ECoG data and compared the behavior of these characteristics on segments containing seizures to interictal segments. As a result, the accumulated energy curve showed no divergence from interictal curves. Distinctive increases in the accumulated energy slope occurred sometime at or after seizure onset for some seizures. Similarly, windowed average power showed no consistent increases in broadband energy before seizures. However, it demonstrated the detection ability for some seizures.

Our results also showed increasing signal variance before the seizure onsets. Increasing signal variance appears to be one of the early warning signals of critical transitions [41]. According to the literature, the *critical transition* is a general definition of the change in the system state passing the bifurcation point. The bifurcation point corresponds to a *critical threshold*. When the dynamical system gets close to the critical threshold, it is referred to as a *critical slowing down*. The bifurcation theory implies that, as the system approaches a *critical threshold*, it becomes slow in recovering from small perturbations. If the small perturbation evolves as  $\sim e^{\lambda t}$ , the dominant eigenvalue  $\lambda$  tends to zero. As the eigenvalue approaches zero, the impacts of perturbations do not decay, and their accumulating effect increases the variance of the state variable.

Other studies also found signs of critical transition before the seizure onset. Meisel and Kuehn analyzed preictal states in the different levels [54]. On the single-neuron level, they employed a model-based analysis with the FitzHugh-Nagumo model and showed that the variance could be a precursor of spiking. On the level of neuronal clusters, they used ECoG data. They observed that the variance demonstrated oscillations before the seizure. Furthermore, the inverse of the variance displayed a linear scaling law manifesting Hopf bifurcation. Chang and co-authors reported the onset of seizures due to the progressive loss of neuronal network resilience

governed by the principles of critical slowing [55]. They further suggested that interictal epileptiform discharges play the role of external perturbations and may control this process. In recent work, Maturana and colleagues found signatures of critical slowing down on the short and long time scales [56]. First, they provided strong evidence of critical transitions (increased autocorrelation and variance) close to the seizure onset. Then, they demonstrated how the measures of critical slowing down (autocorrelation and variance) fluctuated over temporally extended scales (hours to days) and used them to forecast seizures.

In the literature, increased signal variance before seizures has contrasting evidence. While Scheffer *et al.* associated the increased variance as a marker of the critical slowing down, they also mentioned an opposite effect of the critical slowing down on the variance [41]. Different studies pointed out that the early warning signals might describe only a subgroup of critical transitions. Sometimes, shifts may occur without warning. For instance, in a bistable domain, the noise might push the system across the separatrix to the other state. This noise-induced transition does not involve any gradual change of variance. According to Milanowski and Suffczynski, the type of seizure may also define the presence of the early warning signals. Seizures whose type was unknown tended to behave according to the theory, exhibiting an increase in variance before an onset. On the contrary, the decreased variance preceded the seizures classified as complex partial [57]. In recent work, Wilkat, Rings, and Lehnertz reported no evidence for critical slowing down before human epileptic seizures [42]. They supposed that associating a preictal state with critical slowing down might be too simplistic for the human epileptic brain. They also mentioned other potential mechanisms behind this phenomenon, such as noise-induced and rate-dependent tipping. Neither of these requires any change of stability, and there may be no easily identifiable early warning signals for such cases.

The literature provides contradicting evidence about the onset mechanism. Some studies support the concept of critical slowing, while other studies suggested other mechanisms, e.g., noise-induced transition in a bistable domain. In the first case, the early warning signals may precede the onset, while there may be no early warning signals in the latter case. At the same time, noise amplification may subserve the transitions in both cases. During the critical slowing, the noise perturbs the system state. These perturbations do not decay near the critical threshold, and their accumulating effect causes noise amplification. In a bistable domain, where the noise may push the system to the other state, growing noise intensity increases the possibility of such transitions. Here, we demonstrated a strong positive correlation between the noise intensity and the variance. It allowed us to suppose that the variance might increase due to noise amplification, supporting the concept of critical slowing. We did not report a causal relation, but it might be a subject of further studies.

Our study has potential limitations. The number of participants is small; therefore, there is a risk that their individual characteristics influence brain activity. The number of seizures is also small. Thus, there is a risk that the brain state changes over the long time scales affecting the onset mechanisms of the individual episodes. Although experts have marked

the seizure onset, it does not mean that the marked position is the exact point of bifurcation. Finally, our results show that noise intensity increased towards the seizure onset for seven subjects and decreased for three subjects. The variance increased towards the seizure onset for six subjects and decreased for four subjects. Due to a small number of subjects, it is difficult to confidently conclude whether the probability of preictal increase is higher than that of decrease (as the critical transition theory suggests). To test whether the probability of increase and decrease is different, one can use the binomial test and reject  $H_0$ , which assumes equal probability. Considering the probability of increase under  $H_0$  to be  $P = 0.5$ , for  $n = 10$  subjects, the cumulative probability of getting seven increases or more is 0.171. The  $p$ -value of the test is twice

this value, i.e., 0.343. Hence, based on the binomial test,  $H_0$  cannot be rejected, meaning that the probability of preictal increase and decrease is the same. Thus, while the correlation analysis results are positive, the question of a preictal increase in noise intensity remains ambiguous. Next studies should include a larger sample size to provide further support for our hypothesis.

#### ACKNOWLEDGMENT

This work has been partially supported by the President program for Russian Leading Scientific School (Grant No. NSH-2594.2020.2).

- 
- [1] H. L. D. de S. Cavalcante, M. Oriá, D. Sornette, E. Ott, and D. J. Gauthier, *Phys. Rev. Lett.* **111**, 198701 (2013).
- [2] M. Ghil, P. Yiou, S. Hallegatte, B. Malamud, P. Naveau, A. Soloviev, V. Keilis-Borok, D. Kondrashov, V. Kossobokov, O. Mestre *et al.*, *Nonlinear Processes Geophys.* **18**, 295 (2011).
- [3] S. Albeverio, V. Jentsch, and H. Kantz, *Extreme Events in Nature and Society* (Springer, Berlin, 2006).
- [4] C. Nicolis, V. Balakrishnan, and G. Nicolis, *Phys. Rev. Lett.* **97**, 210602 (2006).
- [5] S. L. Kingston, K. Thamilmaran, P. Pal, U. Feudel, and S. K. Dana, *Phys. Rev. E* **96**, 052204 (2017).
- [6] A. Chabchoub, N. Hoffmann, M. Onorato, A. Slunyaev, A. Sergeeva, E. Pelinovsky, and N. Akhmediev, *Phys. Rev. E* **86**, 056601 (2012).
- [7] C. Liu, R. E. Van Der Wel, N. Rotenberg, L. Kuipers, T. F. Krauss, A. Di Falco, and A. Fratalocchi, *Nat. Phys.* **11**, 358 (2015).
- [8] J. M. Dudley, F. Dias, M. Erkintalo, and G. Genty, *Nat. Photonics* **8**, 755 (2014).
- [9] P. Walczak, S. Randoux, and P. Suret, *Phys. Rev. Lett.* **114**, 143903 (2015).
- [10] V. Kishore, M. S. Santhanam, and R. E. Amritkar, *Phys. Rev. Lett.* **106**, 188701 (2011).
- [11] N. Boers, B. Bookhagen, H. M. Barbosa, N. Marwan, J. Kurths, and J. Marengo, *Nat. Commun.* **5**, 1 (2014).
- [12] K. Lehnertz, in *Extreme Events in Nature and Society* (Springer, Berlin, 2006), pp. 123–143.
- [13] I. Osorio, M. G. Frei, D. Sornette, J. Milton, and Y.-C. Lai, *Phys. Rev. E* **82**, 021919 (2010).
- [14] C. B. Field, V. Barros, T. F. Stocker, and Q. Dahe, *Managing the Risks of Extreme Events and Disasters to Advance Climate Change Adaptation: Special Report of the Intergovernmental Panel on Climate Change* (Cambridge University Press, Cambridge, U.K., 2012).
- [15] L. Kuhlmann, K. Lehnertz, M. P. Richardson, B. Schelter, and H. P. Zaveri, *Nat. Rev. Neurol.* **14**, 618 (2018).
- [16] G. D. Hammer and S. J. McPhee, *Pathophysiology of Disease: An Introduction to Clinical Medicine 7/E* (McGraw-Hill, New York, 2014).
- [17] E. M. Goldberg and D. A. Coulter, *Nat. Rev. Neurosci.* **14**, 337 (2013).
- [18] P. Gloor and R. Fariello, *Trends Neurosci.* **11**, 63 (1988).
- [19] G. Nicolis and C. Nicolis, *Foundations of Complex Systems: Emergence, Information and Prediction* (World Scientific, Singapore, 2012).
- [20] N. S. Frolov, V. V. Grubov, V. A. Maksimenko, A. Lüttjohann, V. V. Makarov, A. N. Pavlov, E. Sitnikova, A. N. Pisarchik, J. Kurths, and A. E. Hramov, *Sci. Rep.* **9**, 1 (2019).
- [21] P. Bak, C. Tang, and K. Wiesenfeld, *Phys. Rev. Lett.* **59**, 381 (1987).
- [22] R. Corbalán, J. Cortit, A. N. Pisarchik, V. N. Chizhevsky, and R. Vilaseca, *Phys. Rev. A* **51**, 663 (1995).
- [23] G. Huerta-Cuellar, A. N. Pisarchik, A. V. Kir'yanov, Y. O. Barmenkov, and J. del Valle Hernández, *Phys. Rev. E* **79**, 036204 (2009).
- [24] A. N. Pisarchik, O. N. Pocheppen, and L. A. Pisarchyk, *PLoS One* **7**, e46582 (2012).
- [25] V. Stolbova, E. Surovyatkina, B. Bookhagen, and J. Kurths, *Geophys. Res. Lett.* **43**, 3982 (2016).
- [26] J. S. Ebersole and T. A. Pedley, *Current Practice of Clinical Electroencephalography* (Lippincott Williams and Wilkins, Philadelphia, 2003).
- [27] H. Lüders and S. Noachtar, *Atlas and Classification of Electroencephalography* (Saunders, Philadelphia, 2000).
- [28] A. Hyvärinen and E. Oja, *Neural Networks* **13**, 411 (2000).
- [29] R. Vigário, J. Sarela, V. Jousmiki, M. Hamalainen, and E. Oja, *IEEE Trans. Biomed. Eng.* **47**, 589 (2000).
- [30] G. Kaiser, *A Friendly Guide to Wavelets* (Springer, Berlin, 2010).
- [31] S. Mallat, *Daubechies' Ten Lectures on Wavelets* (Society for Industrial and Applied Mathematics, Philadelphia, 1992).
- [32] A. N. Pavlov, A. E. Hramov, A. A. Koronovskii, E. Y. Sitnikova, V. A. Makarov, and A. A. Ovchinnikov, *Phys. Usp.* **55**, 845 (2012).
- [33] S. V. Bozhokin and I. B. Suslova, *Biomed. Signal Process. Control* **10**, 34 (2014).
- [34] A. E. Hramov, A. A. Koronovskii, V. A. Makarov, A. N. Pavlov, and E. Sitnikova, *Wavelets in Neuroscience* (Springer, Berlin, 2015).
- [35] V. Grubov and V. Nedaivozov, *Tech. Phys. Lett.* **44**, 453 (2018).
- [36] B. Gnedenko, *Ann. Math.* **44**, 423 (1943).
- [37] H. Rinne, *The Weibull Distribution: A Handbook* (CRC Press, Boca Raton, FL, 2008).

- [38] B. J. West and M. Shlesinger, *Am. Sci.* **78**, 40 (1990).
- [39] E. Milotti, [arXiv:physics/0204033](https://arxiv.org/abs/physics/0204033).
- [40] H. Wong, *Microelectron. Reliab.* **43**, 585 (2003).
- [41] M. Scheffer, J. Bascompte, W. A. Brock, V. Brovkin, S. R. Carpenter, V. Dakos, H. Held, E. H. Van Nes, M. Rietkerk, and G. Sugihara, *Nature* **461**, 53 (2009).
- [42] T. Wilkat, T. Rings, and K. Lehnertz, *Chaos* **29**, 091104 (2019).
- [43] J. Bakdash and L. Marusich, *Front. Psychol.* **8**, 1 (2017).
- [44] A. A. Balkema and L. De Haan, *Ann. Probab.* **2**, 792 (1974).
- [45] J. Pickands III *et al.*, *Ann. Stat.* **3**, 119 (1975).
- [46] G. Ansmann, R. Karnatak, K. Lehnertz, and U. Feudel, *Phys. Rev. E* **88**, 052911 (2013).
- [47] A. N. Pisarchik, R. Jaimes-Reátegui, R. Sevilla-Escoboza, G. Huerta-Cuellar, and M. Taki, *Phys. Rev. Lett.* **107**, 274101 (2011).
- [48] D. R. Solli, C. Ropers, P. Koonath, and B. Jalali, *Nature* **450**, 1054 (2007).
- [49] A. Hramov, A. A. Koronovskii, I. Midzyanovskaya, E. Sitnikova, and C. Van Rijn, *Chaos* **16**, 043111 (2006).
- [50] E. Sitnikova, A. E. Hramov, V. V. Grubov, A. A. Ovchinnikov, and A. A. Koronovsky, *Brain Res.* **1436**, 147 (2012).
- [51] P. Suffczynski, F. H. L. Da Silva, J. Parra, D. N. Velis, B. M. Bouwman, C. M. Van Rijn, P. Van Hese, P. Boon, H. Khosravani, M. Derchansky *et al.*, *IEEE Trans. Biomed. Eng.* **53**, 524 (2006).
- [52] B. Litt, R. Esteller, J. Echazu, M. D'Alessandro, R. Shor, T. Henry, P. Pennell, C. Epstein, R. Bakay, M. Dichter *et al.*, *Neuron* **30**, 51 (2001).
- [53] M. A. F. Harrison, M. G. Frei, and I. Osorio, *Clin. Neurophysiol.* **116**, 527 (2005).
- [54] C. Meisel and C. Kuehn, *PLoS One* **7**, e30371 (2012).
- [55] W.-C. Chang, J. Kudlacek, J. Hlinka, J. Chvojka, M. Hadrava, V. Kumpost, A. D. Powell, R. Janca, M. I. Maturana, P. J. Karoly *et al.*, *Nat. Neurosci.* **21**, 1742 (2018).
- [56] M. I. Maturana, C. Meisel, K. Dell, P. J. Karoly, W. D'Souza, D. B. Grayden, A. N. Burkitt, P. Jiruska, J. Kudlacek, J. Hlinka *et al.*, *Nat. Commun.* **11**, 1 (2020).
- [57] P. Milanowski and P. Suffczynski, *Int. J. Neural Syst.* **26**, 1650053 (2016).